Presented at the Society for Experimental Mechanics Annual Conference and Exposition, Portland OR, June 4-6, 2001

Measurement of Residual Stress in MEMS to Sub Megapascal Accuracy

Michael. S. Baker, Maarten P. de Boer, Norman F. Smith and Michael B. Sinclair
Sandia National Laboratories, P.O. Box 5800
Albuquerque, NM, 87185, USA
http://www.mdl.sandia.gov/Micromachine

Abstract

A methodology has been developed to reliably determine the residual stress levels in microelectromechanical systems (MEMS) to ± 0.5 MPa accuracy. The technique relies on measuring the full deflection path of fixed-fixed beams that are electrostatically deflected towards the substrate. Validation of the residual stress values is achieved by taking multiple independent measurements, at different values of the applied load. Information on boundary conditions is also extracted from these curves without the need to resort to finite-element analysis. We show that residual stress values vary across a portion of the wafer by less than approximately 2 MPa for three levels of polysilicon in our five layer surface micromachining technology.

Introduction

An understanding of the thin film material properties in a MEMS process is essential for detailed design and analysis. It is also important for process control as these properties can vary from lot to lot and across a single wafer. Important properties include stress gradient and residual stress. Many deposition parameters including doping levels, thermal conditions, impurities, grain growth and orientation influence these properties [1-3]. Researchers have developed several passive test structures that deflect in some way due to residual stress. This deflection can be measured and used to quantify the stress level. In-plane deflection techniques include pointer structures [4] and bent-beam sensors [5]. They are limited in their resolution by in plane measurement techniques and can be subject to out-of-plane buckling that the analysis does not take into account. Out-of-plane devices include microrings [6] and fixed-fixed beam structures [7,8]. These devices require an array of structures of different lengths and use a transition from flat to buckled as a measure of the stress. However, because boundaries in MEMS are compliant, this transition is not abrupt and therefore difficult to determine. Electrical pull-in and nano-indentation of fixed-fixed beams have also been reported [9,10], but assume that a model can fit a single data point. If non-idealities exist that are different from those modeled, erroneous values can result.

For process control purposes in MEMS, a material property measurement method must allow for rapid property extraction. The test devices should not require a large area since they need to be fabricated in each die location on the wafer. The resolution and accuracy of the measurement technique must also be better than the expected variation in the process being measured. The previously suggested methods are not able to resolve property measurements to the necessary degree of accuracy, especially for the low stress films more commonly encountered in current MEMS processes. Also, several non-idealities, such as film curvature, out-of-plane deflections and support-post compliance, are not normally accounted for and can have a significant influence on the measured values.

Interferometry for Material Property Measurement in MEMS (IMaP) is a technique that uses out-of-plane deflection measurements of electrostatically-actuated cantilevered and fixed-fixed beam test structures to determine material properties. It has been demonstrated to work for measurements of Young's Modulus, stress gradient, residual stress, adhesion and fracture strength [11-14]. The deflection profile is measured along the full length of the beam using an interferometer to within approximately 10 nm resolution. Material properties are then determined by finding the best fit of a finite-difference model to the measured deflection curve. The complete deflection information allows for the support-post compliance to be quantified, improving resolution of the extracted properties. We are working to automate this technique for wafer-level measurement, making it suitable for process monitoring [15].

This paper will explore the accuracy of this method as it is applied to the measurement of residual stress in the Sandia National Laboratories five-level polycrystalline silicon (polysilicon) surface micromachining process [16]. By measuring deflections under an electrostatic load, either compressive or tensile residual stresses can be measured. With 10 nm resolution beam deflection measurements from interferometry, the inherent resolution of each stress measurement is approximately 0.03 MPa. However, the absolute accuracy of each measurement is affected by the non-idealities that must be accounted for in the model. Based on the repeatability seen in the final measurements, the overall accuracy of the method is judged to be within ± 0.5 MPa.

Measurement Methodology

The determination of residual stress is a four-step process. First, the beam geometry must be determined. Specifically, the film thickness and gap between the beam and the substrate must be measured. Second, the fixed-fixed beam deflection curves are measured for several different beam load voltages. Third, the stress gradient through the film thickness is determined by measuring the curvature in adjacent released cantilevered beams. Finally, using the previously measured parameters as inputs, the best fit is found between a finite-difference beam model and the measured deflection curve to determine the residual stress. An important part of this step is quantifying the support-post

compliance. We propose here a method that does not require FEM analysis of the supports.

1. Beam Geometry

The deflection of a fixed-fixed beam due to the internal residual stress and applied voltage is strongly dependent on the film thickness and gap between the beam and the substrate. Because it is bending out of plane, the beam stiffness is a function of the thickness to the third power. With applied voltages, the electrostatic force is a function of the gap squared. As such, it is important that these two parameters be measured accurately. For this study, measurements were made using a calibrated Tencor P-10 Surface Profilometer with an estimated accuracy of ± 0.02 μm. Gap measurements were verified interferometrically by measuring the deflection of a pulled-in cantilevered beam structure adjacent to the fixed-fixed beams. The beam length and width are also necessary parameters and were determined from the mask layout. Because the beams are relatively large compared to the minimum feature size in the process, these dimensions are sufficiently accurate.

2. Fixed-Fixed Beam Deflection Curve

The out-of-plane beam deflection curve can be determined by analyzing the fringe information along the beam length when viewed with an interferometric microscope. Each fringe corresponds to a vertical deflection equal to ½ the wavelength of the light used. In this study, a coherent laser light source was used with a wavelength of 532 nm. Figure 1 is an image of a 1000 μm long beam showing the fringe information along the length of the beam. An intensity linescan is recorded along the beam length and analyzed to determine the beam deflection as shown in Figure 2. The length of the beam in microns is divided by its length in pixels to determine a calibration scale factor (microns/pixel). Beam deflections are measured at several voltages for each beam length. Taking numerous independent measurements allows for verification of the measured stress and is necessary to determine the support compliance.

3. Stress Gradient

A stress gradient through the thickness of a film will cause it to curve out of plane. It is important in design and analysis to know this curvature so that its impact on a design can be accounted for. The film curvature is also an important measure of process control. Because it affects the out-of-plane deflection of fixed-fixed beams, it must be quantified before any additional analysis can be performed.

In any small localized region on a wafer, the stress gradient in the film is assumed to be constant. This assumption has been verified by comparing the curvature in adjacent cantilevered beams. However, the stress gradient does change across an entire wafer so measurements should be made using cantilevered beams located near the fixed-fixed beams of interest. Cantilevered beams can be used for both Young's Modulus and curvature measurements [12].

Stress gradient is determined by measuring the curvature of cantilevered beams. The beam deflection curve is measured using the same method described for the fixed-fixed beams, and the curvature is then directly extracted from the beam

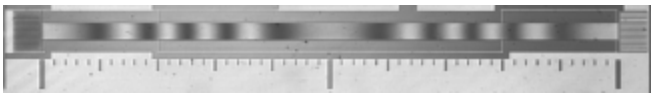

Figure 1 – Interferogram illustrating fringe information (Poly3, L=1000 μm, 0 V).

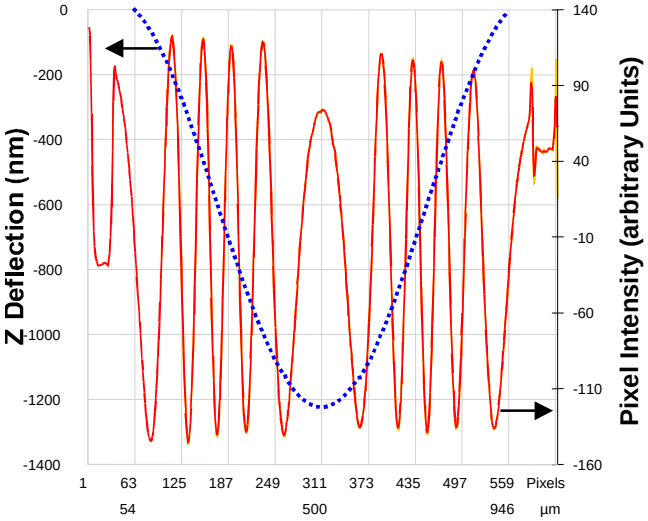

Figure 2 – Linescan and corresponding calculated beam deflection for beam shown in Figure 1.

shape. By using cantilevered beams that are only actuated along a small portion of their length near the support post, this measurement is taken at several voltages to increase the confidence in the extracted curvature value. Only the unactuated portion of the beam is analyzed to determine the curvature. Stress gradient is determined from $E\,k$ where E is Young's Modulus and k is the curvature.

4. Residual Stress

The deflection amplitude of a loaded fixed-fixed beam is highly sensitive to residual stress in the beam. Because of this relationship, the amplitude can be used to determine the magnitude of the residual stress. This is done by varying the residual stress value in a fixed-fixed beam model until the best fit is found between the predicted model deflection and the measured deflection shape.

Several non-idealities must be accounted for in the beam model in order to improve the accuracy and resolution of the results. First, the stress gradient must be included in the model as it affects the beam deflection. Next, in an ideal model, the supports are assumed to be perfectly rigid and the angle of the beam at the support is assumed to be zero. For built-up surface micromachined supports this is not the case. The support will have torsional and axial compliance that will cause it to deflect due to the moment and axial force applied to it as the fixed-fixed beam is deflected. This compliance must be accounted for to accurately determine residual stress. There may also be a non-zero unloaded takeoff angle, q_0, and unloaded axial position, d_0, of the supports due to interactions between residual stress and stress gradient in the support material. Non-zero q_0 and d_0 values can be caused by pad designs in which a highly compressive sacrificial oxide has been completely encased

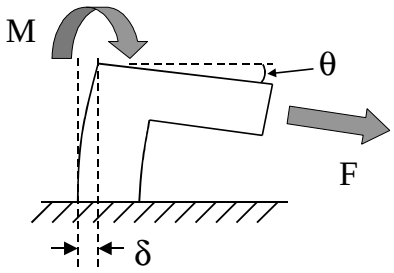

Figure 3 – Support post model.

in polysilicon, preventing it from being removed during the release etch [17].

The axial force and moment applied to the supports by the beam will each contribute to a rotation and an axial deflection. Figure 3 illustrates the support post compliance model we have used for this analysis. By assuming that the support post behaves in a linear elastic manner the loaded takeoff angle, q, is then defined as

$$q = q_0 + b_M \times M + b_F \times F \tag{1}$$

and loaded axial displacement, d, as

$$d = d_0 + g_F \times F + g_M \times M \tag{2}$$

where M and F are the moment and axial force applied to the support post by the electrostatically loaded beam, q_0 is the unloaded takeoff angle, and d_0 is the unloaded axial displacement. The torsional compliance of the support is defined by the compliance constants b_M and b_F, and the axial compliance is defined by the constants g_F and g_M.

To fully characterize the supports, the compliance constants and initial unloaded values for both q and d must be determined. The loaded takeoff angle, q, has a strong effect on the shape of the deflected beam. Because we are recording deflection data along the length of the beam, q can be determined. Both the residual stress and q are varied when finding the best fit of the model to the measured data. This two-parameter fit is found using a quasi-Newton optimization algorithm to minimize the RMS error per pixel between the predicted model deflection and the measured beam deflection.

A contour plot showing the calculated error per pixel for a range of takeoff angle and residual stress values is shown in Figure 4. Typical best fits have an RMS error per pixel of approximately 5 nm/pixel.

The relationship between the takeoff angle and the applied loads can now be characterized by analyzing beams of several different lengths, with several voltages applied at each length. For each of these measurements, q, F, and M are known from the optimized finite-difference solution. The torsional compliance constants, b_M and b_F, as well as the unloaded takeoff angle, q_0, can be determined by a least squares fit of Eq. (1) to the measured values of q for each data point. With q now defined by fixed values of q_0, b_M, b_F, d_0, g_F and g_M, the original deflection data is then reanalyzed

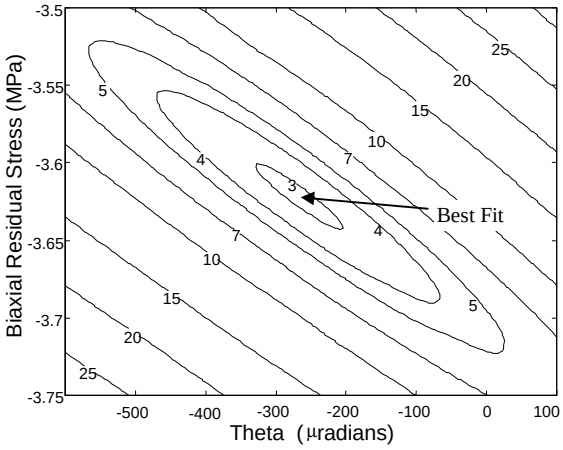

Figure 4 – Contour plot of RMS error per pixel for a range of theta and residual stress. Best fit at 2.9 nm/pixel. (Poly4, L=1000μm, 80V, location 2)

by varying only the residual stress. This second analysis acts to reduce the non-systematic noise in the data, but does not significantly change the average measured residual stress value.

Based on finite-element analysis, the loaded axial deflection of the supports, (d- d_0), is as much as 1 nm, depending on the applied load, beam length, and biaxial residual stress. The change in the measured biaxial stress for a given axial displacement, d, can be found by Hooke's Law using the following equation

$$s = \frac{E}{(1-u)} e = \frac{E}{(1-u)} \left(\frac{2d}{L} \right) \tag{3}$$

where E is Young's Modulus and u is poisson's ratio. For a 600 μm long fixed-fixed beam, 1 nm of axial displacement in each support post would introduce an error in the reported biaxial stress of 0.7 MPa if not accounted for. The influence of an axial displacement decreases with longer beams, but it still must be quantified to improve the resolution of the resulting measurements.

Although it is difficult to measure the nanometer scale axial deflection of the supports, reasonable assumptions can be made to the determine the axial compliance constants. First, for linear elastic materials, the Reciprocity Theorem states that the off-diagonal terms in a compliance matrix must be equal [18]. This means that the parameter g_M must be equal to the already measured parameter, b_F. This reduces the number of unknowns in Eq. (2) to only two, g_F and d_0. Second, we assume residual stress is constant in a small localized area. Based on this assumption, the values for d_0 and g_F are found that minimize the standard deviation in the residual stress values for all measurements taken on adjacent beams. The compliance constant g_F reduces the standard deviation for measurements taken at different voltages on each individual beam length, while the unloaded axial displacement d_0 brings the average values for each different beam length closer together. This final analysis improves the accuracy of the results.

Error Sensitivity Analysis

Because the final value for residual stress is dependent on measured values of the thickness, gap, applied voltage, and curvature it is important to quantify the amount by which errors in these measurements will propagate to an error in the final measured stress value. There are also other possible systematic errors in the data collection procedure that can introduce error. When the data is collected, the distance from the beginning of the beam to the first measured data point is recorded and could be off by ± 1 pixel. We call this an x-offset error. Also, the calibration scale factor could be incorrect by as much as two pixels across the beam length. We call this a calibration error. To determine the extent to which all these errors affect the result, a data set was generated with the finite-difference model and then re-analyzed, introducing each of the possible errors individually. The generated data was based on a 600 μm long beam with a residual stress of –3 MPa. Other geometry and beam properties were selected to be representative of the beams examined in this study. The resulting errors in stress are reported in Table 1. These errors are expected to be independent of the magnitude of the residual stress. A total systematic error of ± 0.17 MPa is expected according to an RMS calculation, which can be applied because the errors are independent.

While the systematic errors examined do not have a major influence on the measured value of residual stress, they do significantly alter the extracted support post compliance parameters. Specifically, the systematic errors shift the b and g compliance constants by typically 10%, but in some cases by as much as several hundred percent. This is most commonly due to errors in where the support post/beam interface is defined while collecting the data, causing more or less of the beam to be included as part of the support. However, it was found that these values still serve well as fitting parameters and improve the resolution of the resulting measurement even if their absolute values are not always accurate.

Table 1 – Systematic error tolerances and their effect on the residual stress measurement.

Model Input	Estimated Error	Max Error in Stress (MPa)
Thickness	± 0.02 μm	0.13
Gap	± 0.05 μm	0.07
Curvature	± 0.2 m^{-1}	0.02
Voltage	± (0.02%+24mV)	0.01
X-Offset	± 1 pixel	0.02
Calibration	± 2 pixels	0.08
Total	(RMS Calculation)	± 0.17

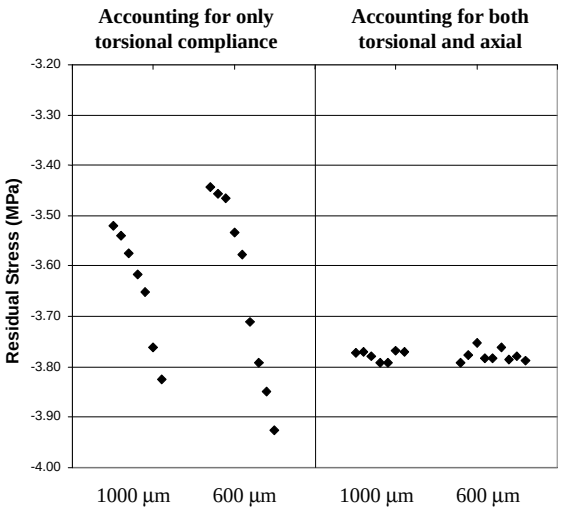

Figure 5 – Comparison before and after accounting for axial compliance for a given beam set. On a given beam, data is shown with voltage increasing to the right. (P4, location 2).

Results

The Sandia National Laboratories surface micromachining process consists of three main structural polysilicon levels, Poly1/Poly2 laminate, Poly3, and Poly4 (P1P2, P3, and P4 respectively). Each of the levels is deposited by LPCVD and annealed at high temperature to reduce the residual stress [16]. Data was collected for each of the three levels at three adjacent locations on a wafer. Layer thickness was uniform across all three locations and was measured as 2.20 μm for P1P2, 2.33 μm for P3 and 2.24 μm for P4. The P1P2 laminate gap was measured as 1.90 μm, and is constant across the wafer. However, the P3 and P4 levels are both deposited after a chemical mechanical polishing (CMP) of the sacrificial oxide layers. This process step is known to induce some cross wafer non-uniformities. The P3 gap ranged from 5.55 μm to 5.60 μm, and the P4 gap ranged from 9.36 μm to 9.63 μm. For the P3 and P4 levels, beam lengths of 600 μm and 1000 μm were examined, but for the P1P2 laminate only the 600 μm length was available. The P1P2 1000 μm beams were buckled down and contacting the substrate, preventing data collection. A value of 165 GPa was used for Young's Modulus [12].

To illustrate the repeatability in the measured values for residual stress, and the effect of taking into account the axial compliance, the measurements for both lengths of P4 at the second wafer location are plotted in Figure 5. For each length, the data points are shown shifted slightly to the right to designate increasing applied voltages. Negative values for residual stress are defined as being compressive. The left two columns show the values that were measured while only taking into account the torsional compliance. The trend in this data shows that the measured residual stress becomes more negative with increased voltage. This is consistent with expectations because the support posts deflect inward at higher voltages. The two right hand columns show this same data after accounting for the axial compliance.

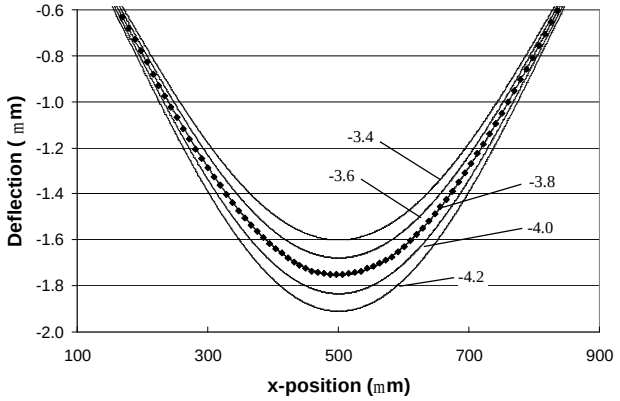

Figure 6 - Model deflections at several residual stress values. The best fit was found at –3.8 MPa with an RMS error of 2.9 nm/pixel. Measured data is shown with dots (every 5th point shown). (P4, L=1000mm, 80V, location 2)

A plot of modeled and measured deflections is shown in Figure 6 for an 80 V load case in P4. The best fit was found at –3.8 MPa with an RMS error of 2.9 nm/pixel. The measured data is shown in the plot with dots, with only every fifth data point included for clarity. Calculated model deflection curves have been included for different stress levels to illustrate the sensitivity of the method to small changes in the residual stress. The same measured support compliance was used for each of these curves.

Summary results for curvature and residual stress for each of the three levels at the three die locations are shown in Figure 7. Positive curvature is defined as curving away from the substrate. From this plot it is clear that both residual stress and the stress gradient vary at different locations on a wafer and at different polysilicon levels. It is interesting to note the similarity between the trends for curvature and residual stress. As the residual stress becomes more positive, so does the curvature. This suggests that the curvature is not completely independent from the value of residual stress. Because of stiction problems, only one curvature measurement could be obtained for the P1P2 layer, so that one value was used in the analysis at each of the other two locations.

Discussion

While the analysis for each polysilicon level at each location on the wafer was tightly grouped (as seen in the right half of Figure 5), there were some trends in the data that were not expected. Before accounting for the axial compliance, the measured residual stress values should become more negative with increasing load due to the axial compliance in the supports. This was seen in many of the data sets examined, but in some cases the stress measurement stopped decreasing and even slightly increased at higher voltages. Also, for some of the deflection measurements, the extracted beam shape was not perfectly symmetric about the center of the beam. We believe both of these errors to be due to some systematic error in the data collection process that is not yet understood or accounted for. Even with the unexpected trends in some of the data sets, the standard

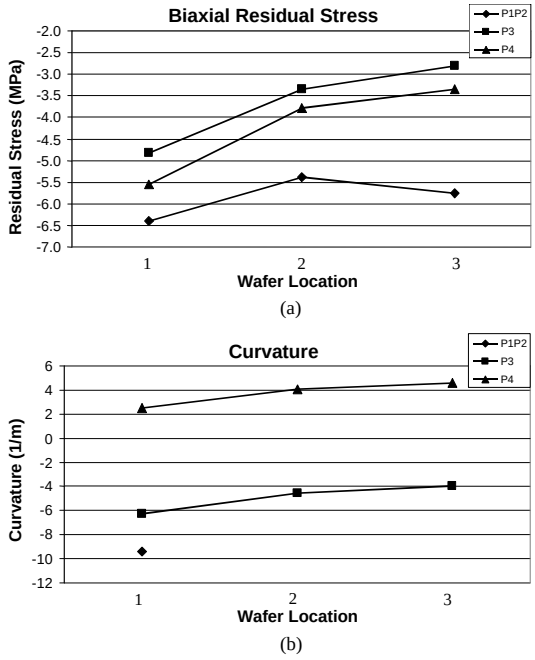

Figure 7 – (a) Biaxial residual stress and (b) curvature at each location and for each level.

deviation before accounting for the axial compliance was less than 0.20 MPa in every case. After adjusting for axial compliance, the standard deviation reduced to less that 0.15 MPa for the worst case, and as low as 0.01 MPa for the best case (Figure 5 shows a final standard deviation of 0.01 MPa). Each polysilicon level, at each wafer location has 15 to 20 independent measurements of residual stress (taken at different voltages and beam lengths). This low standard deviation over a large number of data points suggests that the measurement technique is accounting for most of the significant effects due to non idealities. Based on some of the trends in the data being different from expected, we estimate our current absolute accuracy at ± 0.5 MPa rather than 0.2 MPa.

The method presented in this paper resolves small stress differences across our wafers and offers several advantages for measuring residual stress when compared to other techniques reported in the literature [4-10]. The most important of which is better accuracy with a small sized test structure [19]. In plane bent-beam devices have been demonstrated with a resolution of 1.7 MPa [19], however to achieve this the structures must be large and very compliant. As such, they become very susceptible to out of plane buckling and stiction which reduces their accuracy and reliability. Pointer devices experience the same problems to an even greater degree. Discrete buckling detection techniques, such as the microrings and fixed-fixed arrays, require a large area. To detect stress to within 5% (0.5 MPa) in a range from -1 MPa to -10 MPa, an array of 47 beams would be required [4]. These techniques also do not account for stress gradient or support compliance which cause the buckling event to be continuous and difficult to detect, introducing error in the measurement. Fang and Wickert have achieved very good results using a fixed-fixed beam technique that does account for support compliance [7]. However, our method has the advantage of being able to

provide increased validation through the application of voltage loads. Pull-in voltage measurements detailed in [9] do not account for support compliance or stress gradient, and rely on a single data point for stress determination. While the nano-indentation technique presented in [10] does account for support compliance, it was shown to have a repeatability of only ± 56 MPa (19.2 %) for a film under –291 MPa stress.

Conclusions

Through the use of interferometry, high resolution measurements of actuated beam deflections can be taken. By measuring the deflection along the length of the beam, material properties such as curvature and residual stress were determined with high confidence. Several independent measurements were taken at different voltages and beam lengths for validation of the results. The effect of the known systematic errors has been shown to be small, but the effects of both torsional and axial compliance in the support posts are significant. We have demonstrated a method to take these into account that does not require finite element analysis. This is important for routine measurement. Residual stress values can then be measured to better than ±0.5 MPa accuracy for either compression or tension. Work is under way to advance the current level of automation [15], making it a feasible method for process control on the wafer level.

Acknowledgments

Sandia is a multiprogram laboratory operated by Sandia Corporation, a Lockheed Martin Company, for the United States Department of Energy under Contract DE-AC04-94AL85000.

References

[1] Kamins, T. I., “Design properties of polycrystalline silicon,” *Sensor and Actuators A*, Vol. A23, pp. 817-824, 1990.

[2] Adamaczewska, J., and Budzynsky, T., “Stress in chemically vapour-deposited silicon films,” *Thin Solid Films*, 113 (4), 271, 1984.

[3] Maier-Schneider, D., Koepurueluelue, A., Ballhausen Holm, B., and Obermeier, E., “Elastic properties and microstructure of LPCVD polysilicon films,” *Journal of Micromechanics and Microengineering*, vol. 6, issue 4, pp. 436-446, December 1, 1996.

[4] van Drieënhuizen, B. P., Goosen, J. F. L., French, P. J., and Wolffenbuttel, R. F., “Comparison of techniques for measuring both compressive and tensile stress in thin films,” *Sensors and Actuators A*, Vol. 37-38, 756-765, 1993.

[5] Gianchandani, Y. B. and Najafi, K., “Bent-Beam Strain Sensors,” *Journal of Microelectromechanical Systems*, Vol. 5, No. 1, March 1996.

[6] Guckel, H., Burns, D., Rutigliano, C., Lovell, E., and Choi, B., “Diagnostic microstructures for the measurement of intrinsic strain in thin films*,” Journal of Micromechanics and Microengineering*, Vol. 2, No. 2, pp. 86-95, 1992.

[7] Fang, W. and Wickert, J. A., “Post buckling of micromachined beams,” *Journal of Micromechanics and Microengineering*, Vol. 4, No. 3, pp. 115-122, 1994.

[8] Guckel, H. Randazzo, T., and Burns, D. W., “A simple technique for the determination of mechanical strain in thin films with applications to polysilicon,” *Journal of Applied Physics*, Vol. 57, No. 5, pp. 1671-1675, 1985.

[9] Osterberg, P. M., and Senturia, S. D., “M-TEST: A Test Chip for MEMS Material Property Measurement Using Electrostatically Actuated Test Structures,” *Journal of Microelectromechanical Systems*, Vol. 6, No. 2, June 1997.

[10] Zhang, T. Y., Su, Y. J., Qian, C. F., Zhao, M. H., and Chen, L. Q., “Microbridge Testing of Silicon Nitride Thin Films Deposited on Silicon Wafers," *Acta Materialia*, v. 48(#11), pp. 2843-2857, June 30, 2000.

[11] Jensen, B. D., de Boer, M. P., and Miller, S. L., “IMaP: Interferometry for Material Property Measurement in MEMS,” *1999 International Conference on Modeling and Simulation of Microsystems*, pp. 206-209, San Juan, Puerto Rico, 1999.

[12] Jensen, B. D., de Boer, M. P., Masters, N. D., Bitsie, F. and LaVan, D. A., “Interferometry of actuated cantilevers to determine material properties and test structure non-idealities in MEMS,” *Journal of Microelectromechanical Systems,* in press, 2001.

[13] de Boer, M. P. and Michalske, T. A., “Accurate method for determining adhesion of cantilever beams,” *Journal of Applied Physics*, Vol. 86, No. 2, pp. 817-827, 1999.

[14] de Boer, M. P., Jensen, B. D. and Bitsie, F., “A small area in-situ MEMS test structure to measure fracture strength by electrostatic probing,” *SPIE Proceedings*, Vol. 3875, Materials and Device Characterization in Micromachining, Santa Clara, CA, 1999.

[15] de Boer, M. P., Smith, N. F., Masters, N. M., Sinclair, M. B., and Pryputniewicz, E. J., “Integrated Platform for testing MEMS mechanical properties at the wafer scale by the IMaP methodology,” *ASTM Symposium on the Mechanical Properties of Structural Films,* November 15-16, 2000.

[16] Sniegowski, J. J., and de Boer, M. P., “IC-Compatible Polysilicon Surface Micromachining,” *Annu. Rev. Mater. Sci.*, Vol. 30, pp. 299-333, 2000.

[17] Jensen, B. D., Bitsie, F, and de Boer, M. P., “Interferometric measurement for improved understanding of boundary effects in micromachined beams,” *Micromachining and Microfabrication*, SPIE vol. 3875, Santa Clara, CA, Sept 20-22, 1999.

[18] Thomson, W. T. and Dahleh, M. D., *Theory of Vibration with Applications,* pp. 167, Prentice-Hall, 1993.

[19] Masters, N.D., de Boer, M.P., Jensen, B.D., Baker, M.S., and Koester, D., “Side-by-side comparison of passive MEMS residual strain test structures under residual compression*” Mechanical Properties of Structural Films*, STP No. 1413 (S.B. Brown and C.L. Muhlstein), Eds., American Society for Testing and Materials, West Conshohocken, PA, 2000.